A Digital Twin Approach for Stroke Risk Assessment in Atrial Fibrillation Patients

Matteo Falanga[1], Antonio Chiaravalloti[2], Corrado Tomasi[2], Cristiana Corsi[1]

[1]DEI, University of Bologna, Campus of Cesena, Bologna, Italy
[2]Santa Maria delle Croci Hospital, AUSL della Romagna, Ravenna, Italy

Abstract

Atrial fibrillation (AF) patients have a fivefold increased risk of cerebrovascular events, accounting for 15-18% of all strokes. In stroke prevention, the CHA_2DS_2-VASc is an important score for distinguishing patients with a low-risk of stroke. However, there is currently no specific measure available to determine the level of stroke risk. In this study, we propose a digital twin (DT) model of the left atrium (LA) and the application of computational fluid dynamic simulations (CFD) to improve patient-specific stroke risk assessment. Simulations were run on patient-specific dynamic LA models in sinus rhythm (SR) on three groups of subjects: 10 controls, 10 paroxysmal AF (PAR) and 10 persistent AF (PER). Blood velocity and regions prone to thrombogenesis based on endothelial damage were all measured in both the LA chamber and the left atrial appendage (LAA). Following larger-scale testing and classification analysis, the proposed approach could be used to improve stroke risk assessment.

1. Introduction

The most common form of supraventricular arrhythmia worldwide is atrial fibrillation (AF). The population is getting older and more people are living with chronic illnesses, which supports recent estimates [1] of a significantly higher incidence and prevalence of AF and justifies the phrase "epidemic of our century." The risk of cerebrovascular events is five times higher in people with AF; in the medium term, this is due to structural remodelling of the left atrium (LA), which manifests as increasing dilatation of the LA [2] and extension of the left atrial appendage (LAA) [3]. Such structural remodelling results in a change in mechanical function, which causes a chaotic and drastically diminished contractile activity of the cardiac cells [4], compromising blood washout and encourages clot formation, particularly in the LAA.

The CHA_2DS_2-VASc score is commonly employed in clinical settings to assess stroke risk. Although simple to comprehend, relies on a limited set of factors (e.g., age, sex, hypertension, diabetes, congestive heart failure, prior stroke, etc.) rather than the mechanisms underlying thrombus formation. It is advised for use in identifying low-risk patients [5].

Blood flow patterns within the LA and LAA derived using computational fluid dynamic (CFD) simulations can be used to study the mechanisms underlying thrombus development. Previous research demonstrated the ability to simulate realistic LA blood flow 3D patterns using patient-specific dynamic anatomical models, LA displacement derived from imaging data and boundary conditions derived from Doppler acquisition at the pulmonary veins (PVs) and the mitral valve (MV) [6-7].

In this study, we propose a digital twin (DT) model of the LA and the application of CFD simulations to enhance the ability to assess the risk of stroke for a given patient. After determining the blood velocity field, regions that are prone to thrombogenesis and blood stasis were evaluated among three groups of subjects under sinus rhythm (SR) conditions: 10 controls, 10 paroxysmal AF (PAR) and 10 persistent AF (PER). The results were compared between the groups in order to highlight differences and enable a very early identification of potential parameters that could be used to create a new index for stroke risk stratification.

2. Material and Methods

2.1. Patients data

Contrast Enhanced Computed Tomography (CECT) data from a Philips Brilliance 64 CT scanner were obtained in SR. Ten volumes (170 axial slices, 0.4 mm pixel size, 1 mm slice thickness) covering a cardiac cycle from the end of ventricular diastole were reconstructed and used for the following study using retrospective ECG gating. At the MV and PVs, Doppler measurements were also collected.

2.2. Data analysis

Figure 1 illustrates the data processing workflow that we developed. For each patient, the CECT data were handled as follows: ten volumes were reconstructed using retrospective ECG gating, and only the first volume was segmented to define the LA anatomical model. First of all, a volume of interest was established within the 3D acquisition. By detecting the LA contour in 2D space, LA segmentation was performed slice by slice. A rough segmentation was computed for each slice using intensity thresholding: the peak in the image histogram corresponding to the LA was detected to define two thresholds, which were then used to perform a hysteresis segmentation since it provides more flexibility than a single threshold. Following this, the rough LA contour was adjusted by removing spurious regions using a set of morphological opening and closing operators. Finally, the contour was regularized using a curvature-based level set model. The 3D LA structure was then reconstructed using the data resolution and the 2D LA contours in each slice.

Moreover, a few extra procedures were conducted to make the LA anatomical model suitable for CFD simulation; this

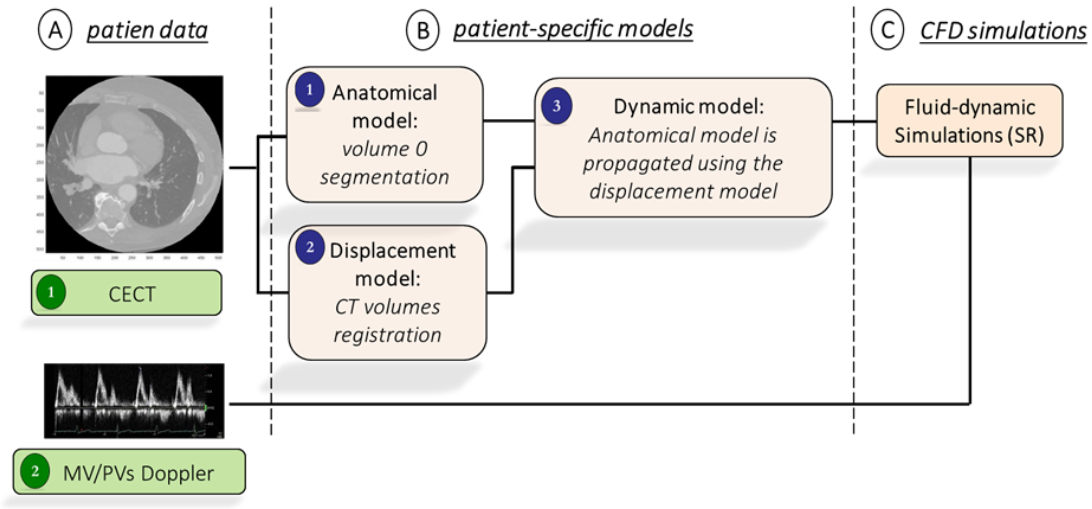

Figure 1: Workflow of the study: patient-specific CECT data (A1) are processed to derive the LA anatomical and displacement models (B1-2) from which a dynamic model (B3) is computed; the latter represents the computational domain for the personalized CFD model (C) using MV/PVs Doppler as boundary conditions (A2).

included employing Laplacian smoothing technique to refine the model and manually adjusting both the inflow (i.e., the four PV's) and outflow (i.e., the MV) planes. After that, a volumetric tetrahedral mesh was created.

To obtain the patient-specific displacement model, CT volume registration and initial mesh propagation were performed using Elastix [8]. Together with Transformix, this library allows you to evaluate and then apply the transformation matrix to register the reference volume. A B-spline model was utilized to execute a non-rigid registration and the mean squared difference was used to optimize registration performance. In accordance with the physiological periodicity of the heart motion, Fourier series interpolation was applied, which recovers a continuous and periodic function from the discrete data provided.

Finally, to run fluid-dynamic simulations in SR conditions, the dynamic model was supplied as input to the customized CFD model [6].

The use of the incompressible Navier-Stokes Equations in the Arbitrary Lagrangian Eulerian frame of reference allowed for the replication of blood flow as a fluid. Using realistic boundary conditions that took into account the MV flowrate and the size of each pulmonary vein, CFD simulations were carried out as previously mentioned.

The dynamic viscosity was adjusted to 0.035 poise, the density to 1.06 g/cm3, and the time step to 0.001 seconds. The LifeX package was used to run the simulations [9].

In order to mitigate the impact of the initial fluid velocity conditions on the results, we conducted a simulation with three heartbeats and solely examined the final one. The blood velocity field for both LA and LAA was examined for each model. Additionally, time-average wall shear stress (TAWSS), oscillatory shear index (OSI), relative residence time (RRT) and endothelial cell activation potential (ECAP) indexes were measured.

These variables can, in fact, be used to detect endothelial shear, the development of new tissues and plaques and the promotion of neointimal hyperplasia [10].

First of all, the viscous stress vector exerted by the wall on the fluid was defined:

$$\vec{\tau} = \mu\,[\nabla\vec{u} + (\nabla\vec{u})^T] \cdot \vec{n}$$

where μ is the blood viscosity and $\nabla\vec{u}$ the velocity gradient, while $\vec{n}$ is the unit normal vector drawn from the fluid through the wall.

In general, the normal component of the viscous stress vector can be subtracted from the total viscous stress vector to yield the wall shear stress (WSS) vector, including direction:

$$\overrightarrow{WSS} = \vec{\tau} - (\vec{\tau} \cdot \vec{n})\,\vec{n}$$

The wall's force on the fluid per unit area is expressed by the WSS in a direction along the local tangent plane. The periodicity of the heartbeat allows to calculate an averaged indicator, the TAWSS, which is defined as:

$$TAWSS = \frac{1}{T}\int_0^T \left\|\overrightarrow{WSS}\right\|_2 \, dt$$

where T is the total duration of the simulated cardiac cycles and $\|\cdot\|_2$ is the Euclidean norm of a vector.

Now let's consider the OSI, defined as follows:

$$OSI = \frac{1}{2}\left(1 - \frac{\left\|\int_0^T \overrightarrow{WSS}\, dt\right\|_2}{\int_0^T \left\|\overrightarrow{WSS}\right\|_2 \, dt}\right)$$

This dimensionless indicator provides values in the range [0,0.5] and is higher in places where the WSS varies significantly over the cardiac cycle. The primary factor contributing to elevated OSI values are the shifts in the flow's direction.

Another index is the RRT, defined as follows:

$$RRT = \frac{1}{(1 - 2OSI) * TAWSS}$$

This indicator locates areas of the wall where the shear stress is small and the flow is oscillatory. The blood residence period in close proximity to the wall lengthens due to this hemodynamic environment.

In order to localize regions of the wall exposed to both high OSI and low TAWSS, a new index was proposed by Di Achille et al. [11] using the ratio of these two indices to characterize the degree of 'thrombogenic susceptibility' of the vessel wall. This metric is referred as ECAP:

$$ECAP = \frac{OSI}{TAWSS}$$

Higher ECAP index values will thus correspond to circumstances of high OSI and low TAWSS, indicating endothelial susceptibility. This measure is frequently utilized in the investigation of thrombogenic risk within LAA.

3. Results

In all study subjects, data processing and simulations were feasible. Generally, the control subjects had higher velocity values in both the LA and LAA than the AF subjects.

Regarding blood velocity, the lowest mean velocity within the LAA was found in a PER subject (0,03 m/s), while the biggest mean velocity was found in a control subject (0,14 m/s). On average, the control group showed a higher velocity (0.11 ± 0.03 m/s) as compared to PAR (0.05 ± 0.02 m/s) and PER (0.04 ± 0.02 m/s) groups ($p<0.05$). Additionally, the mean velocity at the LAA ostium was measured, showing a higher value in the control group (0.28 ± 0.05 m/s) as compared to PAR (0.14 ± 0.03 m/s) and PER (0.11 ± 0.04 m/s) groups ($p<0.05$). Overall, the control subjects showed a better washout throughout the cardiac cycle.

The CFD indexes are shown in Figure 2.

The TAWSS map is shown in the 1st row of the figure. It displays an average value that depends on the velocity gradient since it is evaluated as the integral of the WSS across the full cardiac cycle. We found higher TAWSS values at the ostium of the LAA in the control subjects with respect to the AF subjects. In addition, the TAWSS over the entire LAA was also calculated: control subjects showed an average value of 0.78 ± 0.35 Pa, while PAR and PER subjects showed values of 0.28 ± 0.16 Pa and 0.18 ± 0.07 Pa respectively ($p<0.05$). This means that, overall, the velocity gradient was greater in control subjects.

Following the OSI map, reported in the 2nd row of Figure 2. We found higher OSI values both at the ostium and over the entire LAA in the AF subjects (0.25 ± 0.06 and 0.22 ± 0.06, PAR and PER respectively) with respect to the control subjects (0.20 ± 0.07). One probable explanation is the nature of its movement, which allows at first an emptying, and then a filling, reversing the blood direction, throughout one heartbeat. This changes in direction results in high OSI values, and the major changes are clearly visible in the AF subjects, especially at the tip. However, the parameter didn't show significant differences among the groups ($p = 0.2$).

The RRT map is reported in the 3rd row of Figure 2. Higher values were found in the PAR and PER subjects (123.83 ± 143.68 Pa^{-1} and 112.79 ± 97.25 Pa^{-1}, respectively) as compared to the control (9.09 ± 7.66 Pa^{-1}) group ($p<0.05$). This mean that there is a combination of higher oscillations and lower wall shear stress in the AF subjects as compared to the control subjects that may increase the blood's time in close proximity to the wall, allowing particles to deposit there and inducing an inflammatory response in the endothelial cells.

Finally, the ECAP map is shown in the 4th row of Figure 2.

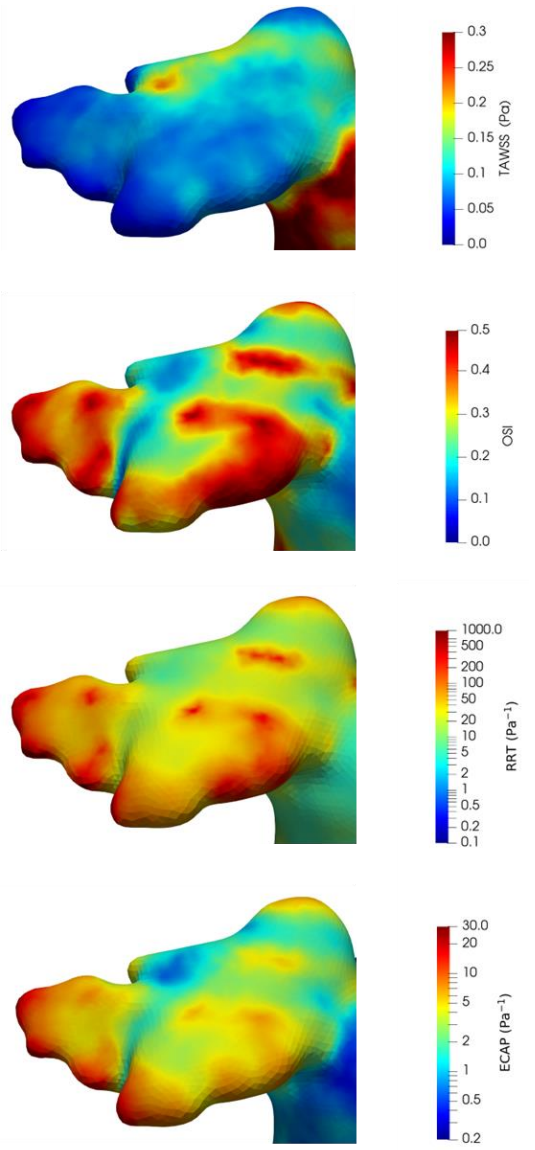

Figure 2: LAA analysis in one PER subject: Time-average wall shear stress (1st row), Oscillatory shear index (2nd row), Relative residence time (3rd row), Endothelial cell activation potential (4th row).

Lower values were found in the control (0.93 ± 0.63 Pa^{-1}) subjects as compared to PAR and PER (4.77 ± 2.08 Pa^{-1} and 3.96 ± 3.28 Pa^{-1}, respectively) subjects ($p<0.5$), suggesting the presence of thrombogenic areas.

4. Discussion

The new method allowed creating a model specifically for each patient using CECT data. Our process could be easily adapted to handle diverse types of data inputs. For example, it could be used with 3D data from other imaging systems such as MRI or real-time 3D echocardiography, as long as the segmentation step is optimized for that particular data.

In recent years, several papers have measured ECAP with the main focus of understanding how specific heart rhythm problems or treatments affect the body and the potential benefits and dangers they may have. Although the studies used different CFD models and methods, the velocity values we found are similar. Unfortunately, comparing ECAP values is more challenging because we need to make the data comparable between different subjects.

By implementing this approach, the CHA_2DS_2-VASc score can be enhanced, enabling personalized blood clot prevention treatment and facilitating doctors in scheduling examinations. To achieve this aim, we need to overcome various challenges in both imaging and modeling areas. Cardiac imaging is an important method for checking for blood clot risks in patients with atrial fibrillation. However, it cannot analyze the reasons why blood clots form, like what happens in the blood vessels and the blood clotting process.

Some studies have found that it is possible to assess a hypercoagulability index of the blood by using a simplified system of reaction-diffusion-convection equations to describe the thrombus growth dynamics. This model is centered around the study of key proteins such as thrombin, fibrinogen, and fibrin [12], which are essential components involved in blood clotting. Our method would greatly benefit from including these extra indicators to get a better understanding of how each factor affects the risk of stroke.

5. Conclusions

In summary, these preliminary results suggest that there are evident disparities between patients diagnosed with AF and individuals who are considered healthy. This means that this method has the potential to assess the risk of stroke in AF patients. We are currently conducting further tests on a larger sample population. In addition, we are also assessing different measurements through our computations. It is crucial to follow these steps in order to validate the authenticity of the initial findings and ascertain the risk level associated with each patient.

Acknowledgments

This work was supported by the Italian Ministry of University and Research (Italian National Project, PRIN2017 ('Modeling the heart across the scales').

References

[1] J. Kornej, C. S. Börschel, E. J. Benjamin and R. B. Schnabel, "Epidemiology of atrial fibrillation in the 21st century: novel methods and new insights," Circulation Research, vol. 127(1), pp. 4-20, June 2020.

[2] D. K. Gupta, A. M. Shah, R. P. Giugliano, C. T. Ruff, E. M. Antman, L. T. Grip, et al., "Left atrial structure and function in atrial fibrillation: Engage af-timi 48," European Heart Journal, vol. 35(22) , pp. 457–1465, 2014.

[3] L. Di Biase, P. Santangeli, M. Anselmino, P. Mohanty, I. Salvetti, S. Gili, et al., "Does the left atrial appendage morphology correlate with the risk of stroke in patients with atrial fibrillation?: results from a multicenter study," Journal of the American College of Cardiology, vol. 60 (6), pp. 531–538, 2012.

[4] S. Yaghi, C. Song, W. A. Gray, K. L. Furie, M. S. Elkind, and H. Kamel, "Left atrial appendage function and stroke risk," Stroke, vol. 46(12), 3554–3559, 2015.

[5] J.J.V. McMurray and al. and the ESC Committee for Practice Guidelines, "ESC Guidelines for the diagnosis and treatment of acute and chronic heart failure 2012: The Task Force for the Diagnosis and Treatment of Acute and Chronic Heart Failure 2012 of the European Society of Cardiology. Developed in collaboration with the Heart Failure Association (HFA) of the ESC," European Heart Journal, vol. 33(14), pp. 1787–1847, July 2012.

[6] A. Masci, M. Alessandrini, D. Forti, F. Menghini, L. Dedè, C. Tomasi, A. Quarteroni, C. Corsi, "A Proof of Concept for Computational Fluid Dynamic Analysis of the Left Atrium in Atrial Fibrillation on a Patient-Specific Basis." J Biomech Eng. vol. 142(1):011002, Jan 2020.

[7] J. Mill, V. Agudelo, C. Hion Li, J. Noailly, X. Freixa, O. Camara, D. Arzamendi, "Patient-specific flow simulation analysis to predict device-related thrombosis in left atrial appendage occluders," REC Interv Cardiol. Vol. 3(4), pp. 278-285, 2021.

[8] S. Klein, M. Staring, K. Murphy, M. A. Viergever and J. P, W. Pluim Elastix: A toolbox for intensity-based medical image registration. IEEE Transactions on Medical Imaging, vol. 29(1), pp.196–205, 2010.

[9] P.C. Africa, "Lifex: a flexible, high performance library for the numerical solution of complex finite element problems", SoftwareX 20, 101252 (2022).

[10] David N. Ku, Don P. Giddens, Christopher K Zarins, and Seymour Glagov. "Pulsatile flow and atherosclerosis in the human carotid bifurcation. Positive correlation between plaque location and low oscillating shear stress". In: Arteriosclerosis, Thrombosis, and Vascular Biology 5 (1985), pp. 293–302.

[11] P. Di Achille, G. Tellides, C. A. Figueroa, and J. D. Humphrey, "A haemodynamic predictor of intraluminal thrombus formation in abdominal aortic aneurysms," vol. 470, no. 2172. Royal Society.

[12] A. Qureshi, M. Balmus, S. E. Williams, G.Y H Lip, D. A. Nordsletten, O. Aslanidi and A. de Vecchi. Modelling Virchow's Triad to Improve Stroke Risk Assessment in Atrial Fibrillation Patients. Computing in Cardiology 2022, vol. 49, pp. 1-4, 2022.

Address for correspondence:

Matteo Falanga
DEI, University of Bologna,
Via dell'Università 50, 47522 Cesena (FC), Italy
matteo.falanga2@unibo.it